Discovery of two Na^+-centered Silverton-type polyoxometalates $\{NaM_{12}O_{40}\}$ (M = Mo, W)

Rong Wan, Zhen Liu, Xinyi Ma, Huafeng Li, Pengtao Ma, Chao Zhang, Jingyang Niu* and Jingping Wang*[a]

[a]Henan Key Laboratory of Polyoxometalate Chemistry, College of Chemistry and Chemical Engineering, Henan University, Kaifeng, Henan 475004, (P. R. China), Fax: (+86)-371-23886876, E-mail: jyniu@henu.edu.cn, jpwang@henu.edu.cn

Content:

Materials and Syntheses

$Na_2MoO_4·2H_2O$, $Na_2WO_4·2H_2O$, Sb_2O_3, $RuCl_3$, Dimethyl sulfoxide (DMSO) and other chemical reagents were acquired from commercial sources and used directly. IR spectra were conducted on a Bruker VERTEX 70 IR spectrometer (KBr pellets) recording in the range of 4000–450 cm^{-1}. Powder X-ray diffraction (PXRD) patterns were obtained by employing a Bruker D8 ADVANCE diffractometer with Cu Kα radiation (the value of λ is 1.54056 Å). TG analyses were measured by a Perkin-Elmer TGA7 instrument under flowing N_2 (heating rate, 10 °C min^{-1}). Elemental analyses (C, H, N) were conducted on an Elementar Vario MICRO analyzer. The vapor adsorption was performed on an automatic volumetric adsorption equipment (BELSORP-max II). Electrospray Ionization Mass Spectrometry (ESI-MS) was detected on a Triple TOF 4600-1 mass spectrometer and all spectra were collected in negative mode. NMR spectra were recorded on a Bruker AVANCE NEO 500 MHz NMR spectrometer with Larmor frequency of 132.26 MHz for ^{23}Na, 32.57 MHz for ^{95}Mo, and 20.81 MHz for ^{183}W. The ^{23}Na, ^{95}Mo, and ^{183}W spectra were referenced (0.00 ppm) to NaCl (1 mol L^{-1}), Na_2MoO_4 (2 mol L^{-1}), and Na_2WO_4 (1 mol L^{-1}) in D_2O, respectively. The UV spectra were recorded with a UH 4150 spectrograph in the range of 800–200 nm in water.

Syntheses of 1 and 2

1: Sb_2O_3 (0.058 g, 0.20 mmol) was completely dissolved in 1 mL 37% HCl and 4 mL water, which then was added into 5 mL aqueous solution containing $Na_2MoO_4·2H_2O$ (0.726 g, 3 mmol) dropwise under stirring. The pH of the solution was adjusted to 5.6 by the dropwise addition of 6 M NaOH. Then, $RuCl_3$ (0.15 g, 0.72 mmol) solution refluxed in 2 mL dmso for 20 min was added into above mixture. Subsequently, the resulting solution was heated to 80 °C for 3 h. The final solution was transferred to a Teflon-lined autoclave and kept in an oven at 120 °C for 24 h, and then cooled to room temperature. Finally, small red block crystals of **1** were obtained. Yield: 55 mg (8.7% based on Ru). Solid **1** was only slightly resolved in H_2O and DMSO, and nearly insoluble in CH_3CN, CH_2Cl_2, $CHCl_3$, CH_3OH, CH_3CH_2OH and DMF. Elemental analysis calcd for **1** (%): H, 2.83; C, 8.26; S, 11.02. Found: H, 3.02; C, 8.00; S, 10.88. TGA (weight loss): the first step 25–283 °C, 6.50% (cald. 6.70%, 13 water molecules); the second step 283–1000 °C, 27.00% (cald. 26.81%, 12 dmso molecules). UV-vis spectrum (H_2O): λ = 230, 340 nm.

2: The synthetic procedure of **2** was similar to **1**, except that $Na_2MoO_4·2H_2O$ (0.726 g, 3 mmol) was replaced by $Na_2WO_4·2H_2O$ (1.52 g, 4.6 mmol), and further $RuCl_3$/DMSO (0.248g, 1.2 mmol; 6 mL) reflowed solution adding in. Finally, a few small yellow green block crystals of **1** and a lot of yellow needle crystal as by-products were obtained. The by-product is cyclic polyoxoanion $[(H_6W_9O_{33})(Ru(dmso)_3)_2]^{2-}$ characterized by single-crystal X-ray diffraction, and the structure of which was same to Kortz's previous work.[1,2] Yield: 54 mg (6.03% based on Ru). Solid **2** can also be slightly resolved in H_2O and DMSO, and nearly undissolved in CH_3CN, CH_2Cl_2, $CHCl_3$, CH_3OH, CH_3CH_2OH and DMF. Elemental analysis calcd for **2** (%): H, 2.17; C, 6.34; S, 8.89. Found: H, 2.30; C, 6.17; S, 8.67. TGA (weight loss): the first step 25–274 °C, 5.38% (cald. 5.14%, 13 water molecules); the second step 274–1000 °C, 20.39% (cald. 20.59%, 12 dmso molecules). UV-vis spectrum (H_2O): λ = 220, 280 nm.

X-ray crystallography

The single crystals **1** and **2** were directly fixed on a loop and kept at 150.0 K during data collection on a Bruker D8 VENTURE PHOTON II CCD diffractometer with Mo Kα radiation (the value of λ is 0.71073 Å), After the data reduction,[3] Olex2 was applied to analyse the structures, by which it was first solved with the ShelXT structure solution program by the utilization of direct methods and then refined with the ShelXL-2018/3 refinement package using least squares minimisation.[4] In addition, all the atoms are refined anisotropically in the final refinement cycle, only few harsh constraints have been used in order to eliminate the ADP alert of few atoms. And some lattice water molecules were located by Fourier map, whereas the rest lattice molecules were determined by TGA results and element analyses. All H atoms on water molecules in the molecular formula were directly included. Crystallographic data of **1** and **2** have been deposited in the Cambridge Crystallographic Data Center with CCDC numbers: 1993610–1993611. Crystal data and structure refinement parameters are detailed in Table S2.

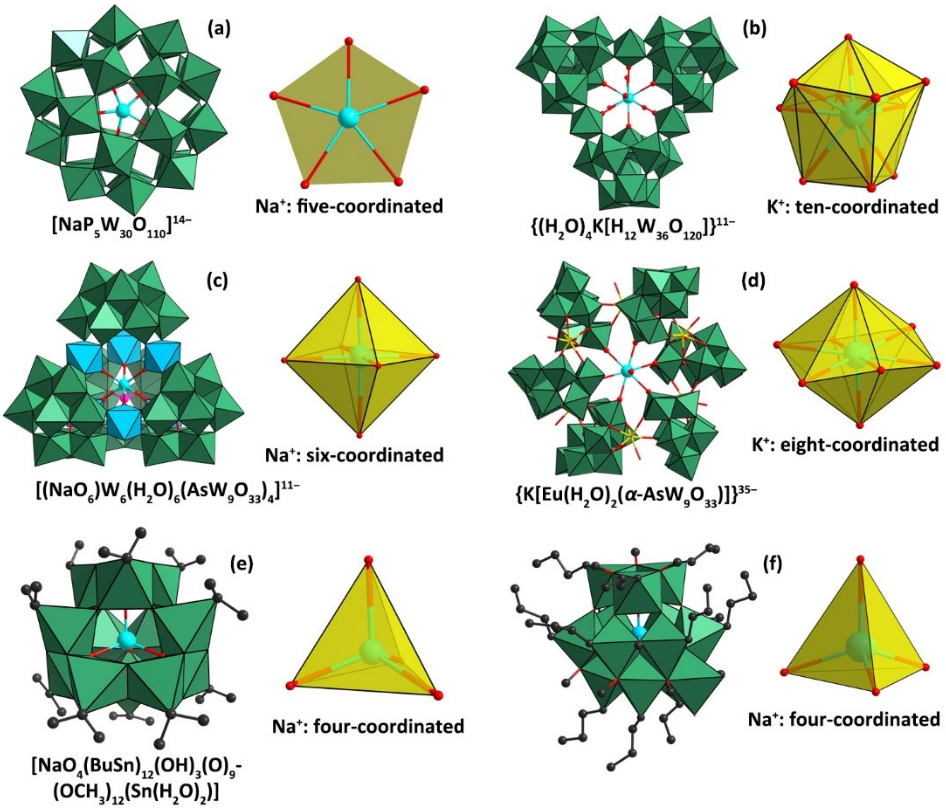

Fig. S1 Representative cluster polyanions and the geometric configurations of their Na^+ and K^+ templates: topical polyoxometalates (a) $[NaP_5W_{30}O_{110}]^{14-}$, (b) $\{(H_2O)_4K\subset[H_{12}W_{36}O_{120}]\}^{11-}$, (c) $[(NaO_6)W_6(H_2O)_6(AsW_9O_{33})_4]^{11-}$, (d) $\{K[Eu(H_2O)_2(\alpha\text{-}AsW_9O_{33})]\}^{35-}$ (S_6); Alkyltin Keggin clusters templated by sodium: (e) $[(i\mathrm{Pr}Sn)_{12}O_4(OH)_{24}][Ag_7I_{11}]\cdot NaCl\cdot H_2O\cdot 10DMSO$ (iPr = isopropyl) (γ-$NaSn_{12}$), and (f) $[NaO_4(BuSn)_{12}(OH)_3(O)_9(OCH_3)_{12}(Sn(H_2O)_2)]$ (β-$NaSn_{13}$).

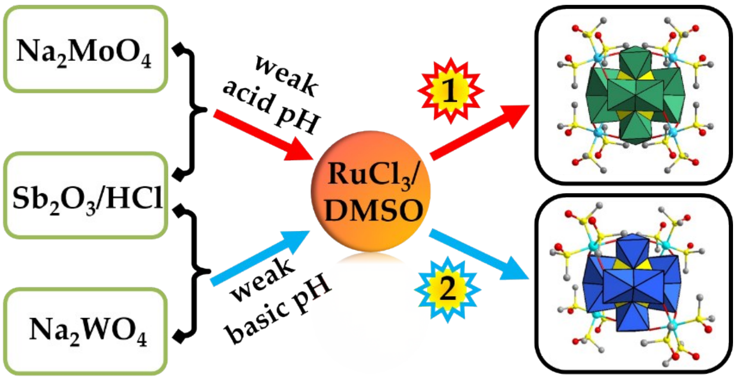

Scheme S1 Synthetic Discussion of the System.

Table S1 Comparation on the features of the reported Silverton-type POMs, **1** and **2**.

Compounds based on Silverton-type polyanion $[XM_{12}O_{42}]^{n-}$	Oxidation state of central metals	Overall charge of the POMs	Dimension	Bond length of Central X–O (Å)	Ref.
$(NH_4)_2H_6[CeMo_{12}O_{42}]·12H_2O$	+VI	8–	0D	2.486–2.494	5
$[Gd(H_2O)_3]_3[GdMo_{12}O_{42}]·3H_2O$	+III	9–	3D	2.494, 2.527	6
$[Nd(H_2O)_3]_3[NdMo_{12}O_{42}]·2H_2O$	+III	9–	3D	2.419–2.552	7
$Mn_7(MnW_{12}O_{42})(OH)_4(H_2O)_8$	+II	10–	3D	2.774	8
$Mg_7(MgW_{12}O_{42})(OH)_4(H_2O)_8$	+II	10–	3D	2.574	9
1	+I	11–	3D	2.574	This work
2	+I	11–	3D	2.567	This work

Table S2 Crystallographic data of **1** and **2**.

	1	**2**
Empirical formula	$H_{98}C_{24}O_{67}Na_4S_{12}Ru_4Mo_{12}$	$H_{98}C_{24}O_{57}Na_4S_{12}Ru_4W_{12}$
Formula weight	3491.29	4546.09
Crystal system	cubic	cubic
Space group	*P-43n*	*P-43n*
a [Å]	17.9058(7)	17.9539(9)
b [Å]	17.9058(7)	17.9539(9)
c [Å]	17.9058(7)	17.9539(9)
α /°	90	90
β /°	90	90
γ /°	90	90
Volume/Å^3	5740.9(7)	5787.3(9)
Z	2	2
ρ_{calc}g/cm^3	1.912	2.502
μ/mm^{-1}	2.076	12.675
F(000)	3176.0	3944.0
Crystal size/mm^3	0.29 × 0.2 × 0.16	0.22 × 0.18 × 0.15
Index ranges	$-21 \le h \le 17$, $-21 \le k \le 21$, $-18 \le l \le 21$	$-13 \le h \le 23$, $-23 \le k \le 23$, $-23 \le l \le 22$
Reflections collected	27490	34516
Data/restraints/ parameters	1705/0/87	2398/0/87
R_{int}	0.0336	0.0582
Goodness-of-fit on F^2	1.180	1.124
R_1, wR_2 [$I \ge 2\sigma(I)$]	0.0464, 0.1145	0.0277, 0.0720
R_1, wR_2 [all data]	0.0510, 0.1223	0.0397, 0.0779

Table S3 Selected bond distances (Å) for polyanions **1a** and **2a**.

Compound	**1**	**Compound**	**2**
Bond	**Length (Å)**	**Bond**	**Length (Å)**
Mo(1)-O(1)	1.870(6)	W(1)-O(1)	1.896(6)
Mo(1)-O(1)^{2}	2.304(8)	W(1)-O(1)^{2}	2.281(9)
Mo(1)-O(1)^{3}	2.188(7)	W(1)-O(1)^{3}	2.167(9)
Mo(1)-O(2)	1.754(8)	W(1)-O(2)	1.782(9)
Mo(1)-O(3)	1.695(8)	W(1)-O(3)	1.703(9)
Mo(1)-O(4)	1.947(5)	W(1)-O(4)	1.939(5)
Ru(1)-S(1)	2.254(3)	Ru(1)-S(1)	2.242(4)
Ru(1)-S(1)^{2}	2.254(3)	Ru(1)-S(1)^{2}	2.242(4)
Ru(1)-S(1)^{4}	2.254(3)	Ru(1)-S(1)^{4}	2.242(4)
Ru(1)-O(2)^{2}	2.074(8)	Ru(1)-O(2)^{2}	2.056(10)
Ru(1)-O(2)	2.074(8)	Ru(1)-O(2)	2.056(10)
Ru(1)-O(2)^{4}	2.074(8)	Ru(1)-O(2)^{4}	2.056(10)
Na(1)-O(1)^{2}; Na(1)-O(1)^{3}; Na(1)-O(1)^{5}; Na(1)-O(1)^{4};Na(1)-O(1)^{6}; Na(1)-O(1); Na(1)-O(1)^{7}; Na(1)-O(1)^{8}; Na(1)-O(1)^{9}; Na(1)-O(1)^{10}; Na(1)-O(1)^{11}; Na(1)-O(1)^{1}	2.574(6)	Na(1)-O(1)^{2}; Na(1)-O(1)^{3}; Na(1)-O(1)^{5}; Na(1)-O(1)^{4};Na(1)-O(1)^{6}; Na(1)-O(1); Na(1)-O(1)^{7}; Na(1)-O(1)^{8}; Na(1)-O(1)^{9}; Na(1)-O(1)^{10}; Na(1)-O(1)^{11}; Na(1)-O(1)^{1}	2.567(6)
Na(2)-O(3)^{3}; Na(2)-O(3)^{6}; Na(2)-O(3)	2.333(10)	Na(2)-O(3)^{3}; Na(2)-O(3)^{6}; Na(2)-O(3)	2.354(11)
Na(2)-O(5)^{12}; Na(2)-O(5)^{13}; Na(2)-O(5)^{14}	2.413(12)	Na(2)-O(5)^{12}; Na(2)-O(5)^{13}; Na(2)-O(5)^{14}	2.385(12)

For **1**: ^{1}2-X,2-Y,+Z; ^{2}+Y,+Z,+X; ^{3}2-Y,2-Z,+X; ^{4}+Z,+X,+Y; ^{5}2-Y,+Z,2-X; ^{6}+Z,2-X,2-Y; ^{7}2-Z,+X,2-Y; ^{8}2-Z,2-X,+Y; ^{9}+X,2-Y,2-Z; ^{10}2-X,+Y,2-Z; ^{11}+Y,2-Z,2-X; ^{12}3/2-Y,1/2+X,3/2-Z; ^{13}3/2-Z,1/2+Y,3/2-X; ^{14}3/2-X,1/2+Z,3/2-Y; ^{15}-1/2+Y,3/2-X,3/2-Z. For **2**: ^{1}-X,-Y,+Z; ^{2}+Y,+Z,+X; ^{3}-Y,-Z,+X; ^{4}+Z,+X,+Y; ^{5}-Y,+Z,-X; ^{6}-X,+Y,-Z; ^{7}+Z,-X,-Y; ^{8}-Z,+X,-Y; ^{9}+Y,-Z,-X; ^{10}+X,-Y,-Z; ^{11}-Z,-X,+Y; ^{12}-1/2-Y,1/2+X,-1/2-Z; ^{13}-1/2-Z,1/2+Y,-1/2-X; ^{14}-1/2-X,1/2+Z,-1/2-Y; ^{15}-1/2+Y,-1/2-X,-1/2-Z

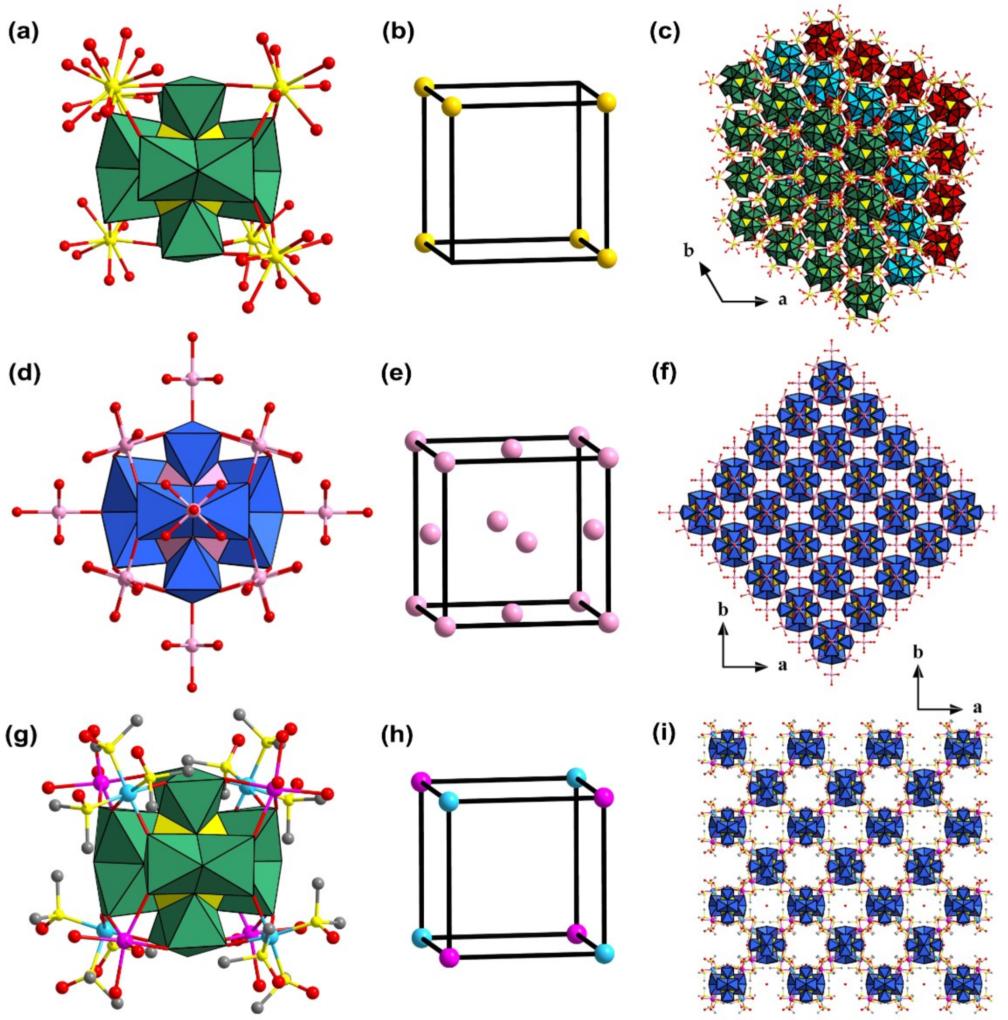

Fig. S2 Comparations of the reported Silverton-type POMs, **1** and **2**. These POM frameworks have displayed practically different 3D packing alignments when using the isostructural Silverton-type polyanions $[XM_{12}O_{42}]^{n-}$ (n = 9–11) as nodes, and all originated in that the final packing modes are sensitive to the linker number, linker types , or the coordinated sites relative to the POM nodes.

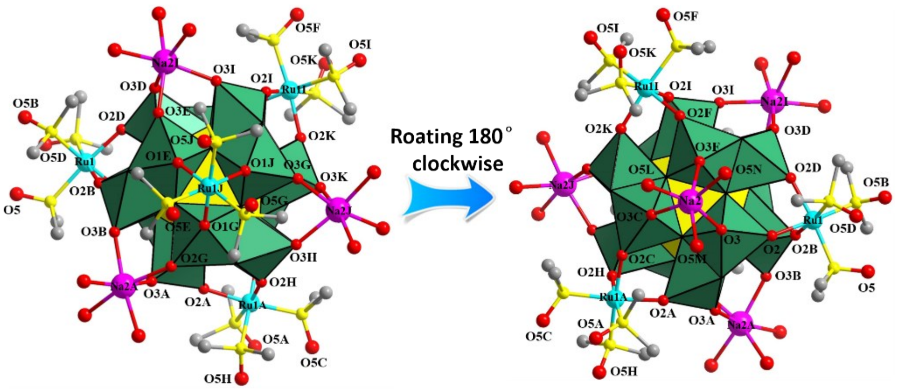

Fig. S3 Combined polyhedral/ball-and-stick representations of polyanions **1a** and **2a**.

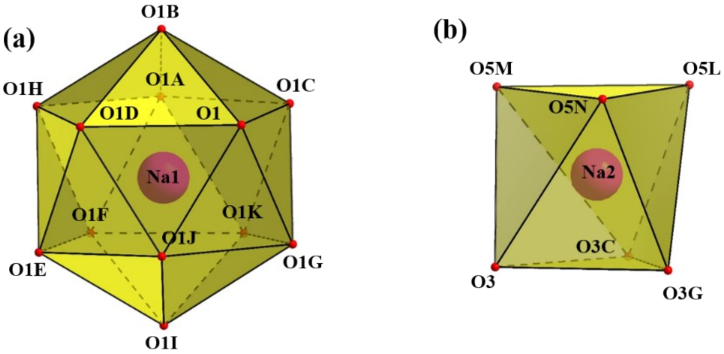

Fig. S4 The coordination geometries of (a) central Na^+ ion in icosahedron configuration and (b) external bridged Na^+ ions in the distorted trigonal antiprism configuration.

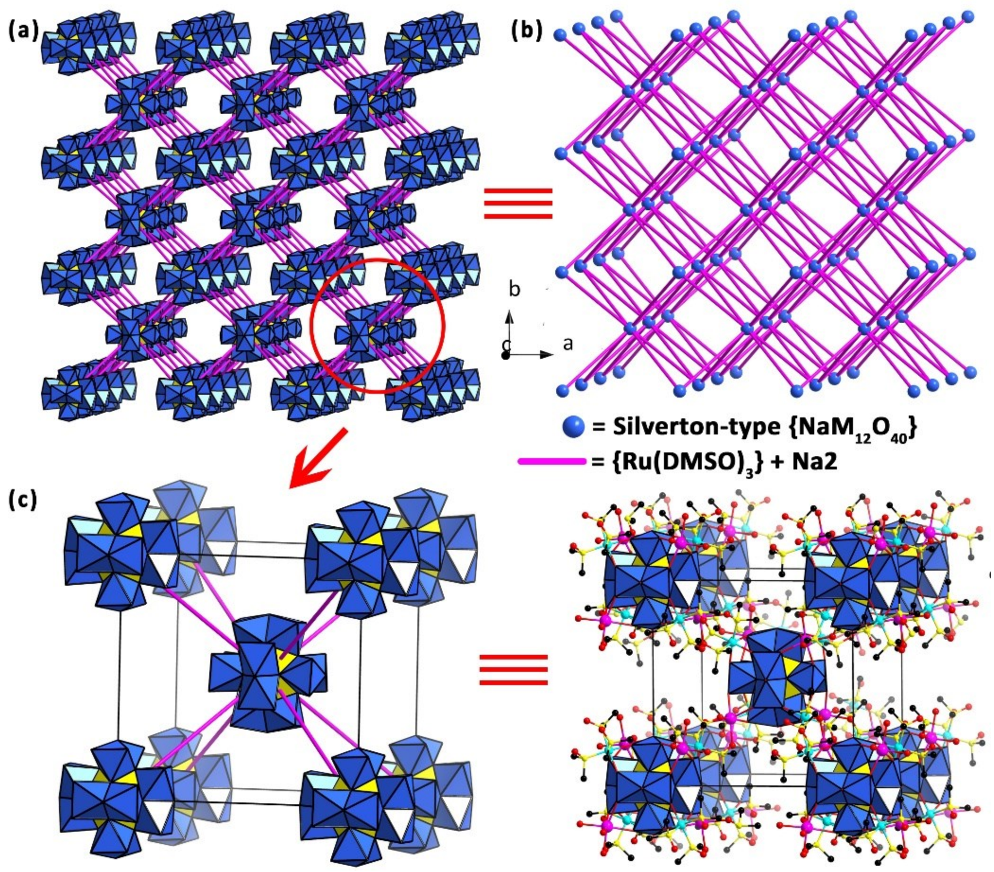

Fig. S5 (a) and (b) Schematic representation of the cubic (bcu) topology of the eight-connected framework of **1** and **2**; (c) Representation of unit cell of **1** and **2:** each SBU (blue circle) of **1** or **2** is connected to eight adjacent SBUs through {Ru(DMSO)3} and Na2 (pink line).

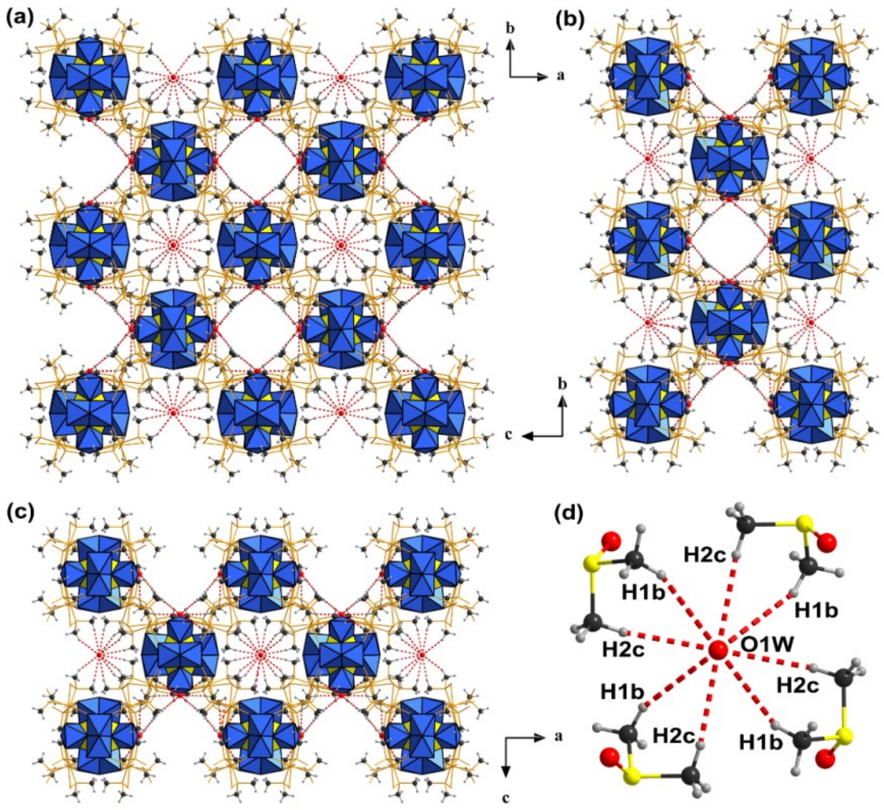

Fig. S6 Hydrogen-bond interactions in **1** and **2**.

Table S4 Lattice parameters of crystals **1** and **2** after soaking in several solvents for 2 days. [a]

Solvent Resistance	**Lattice parameters**	
	1	**2**
Fresh crystals	a=b=c=17.91 Å, α=β=γ=90°, V=5741 Å^3, cubic, *P*-43n	a=b=c=17.95 Å, α=β=γ=90°, V=5787 Å^3, cubic, *P*-43n
CH_3CN	a=b=c=17.85 Å, α=β=γ=90°, V=5692 Å^3, cubic, *P*-43n	a=b=c=17.88 Å, *α=β=γ*=90°, V=5716 Å^3, cubic, *P*-43n
CH_3OH	a=b=c=17.83 Å, α=β=γ=90°, V=5668 Å^3, cubic, *P*-43n	a=b=c=17.88 Å, *α=β=γ*=90°, V=5716 Å^3, cubic, *P*-43n
CH_3CH_2OH	a=b=c=17.92 Å, α=β=γ=90°, V=5752 Å^3, cubic, *P*-43n	a=b=c=17.92 Å, *α=β=γ*=90°, V=5751 Å^3, cubic, *P*-43n

[a]In the case of solvent exchange studies, we take CH_3CN, CH_3OH and CH_3CH_2OH with relatively small volume as examples. After soaking as-prepared crystals **1** and **2** in CH_3CN, CH_3OH and CH_3CH_2OH for 2 days with continuous stirring, we collected their crystallographic data by X-ray single crystal diffraction. The results showed hardly no change was observed in their lattice parameters and XRD patterns (Table S4, Fig. S7), indicating that the two clusters remain stable in these solvents. Additionally, the water molecule was not found to be exchanged by these small

organic solvent molecules after refining the crystallographic data, and also no solvents were absorbed into the empty channel. Due to the abundant hydrogen-bond interaction around them, it is not easy to remove the water molecules. When the fresh crystals **1** and **2** were heated at 150 °C for 6 h in a vacuum oven, both of them were still crystalline phase, which were further characterized by X-ray single crystal diffraction (Crystal data for **1-150°C-6h**: cubic, *P*-43n, $a = b = c = 17.724(5)$; V = 5568(5) Å^3; **2-150°C-6h**: cubic, *P*-43n, $a = b = c = 17.703(4)$; V = 5548(4) Å^3). After refined the data, water molecules were still fixed in the channels across 3D POM frameworks of **1** and **2**. However, the water molecules could be removed by extending the heating time or elevating the heating temperature, but the structures of **1** and **2** destroyed in these two situations as their XRD patterns being changed accordingly (Fig. S8).

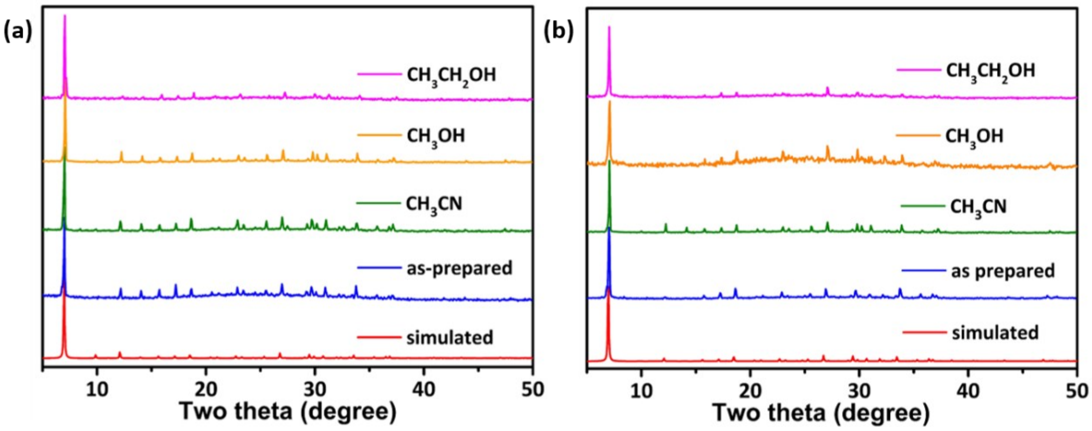

Fig. S7 PXRD patterns: the immersion of (a) **1** and (b) **2** in different solvents for 2 days.

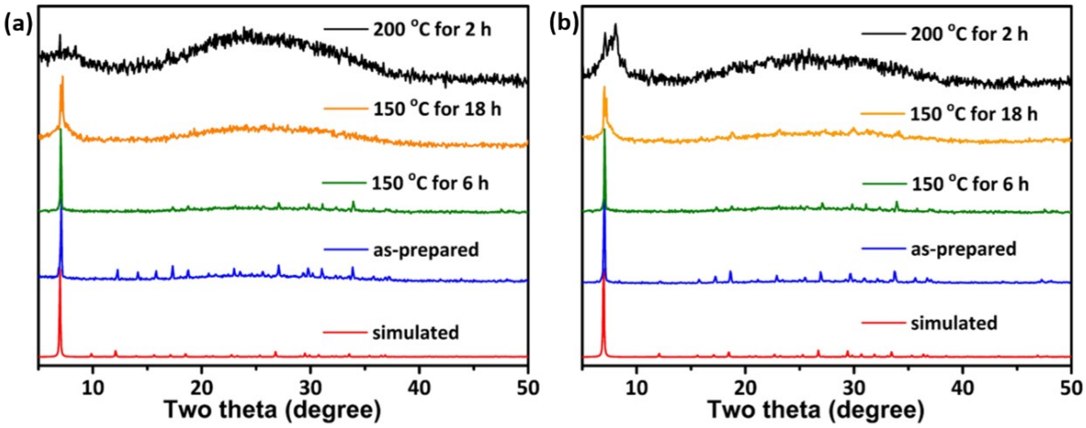

Fig. S8 The PXRD patterns of compound (a) **1** and (b) **2** after heated at different temperature in vacuum oven.

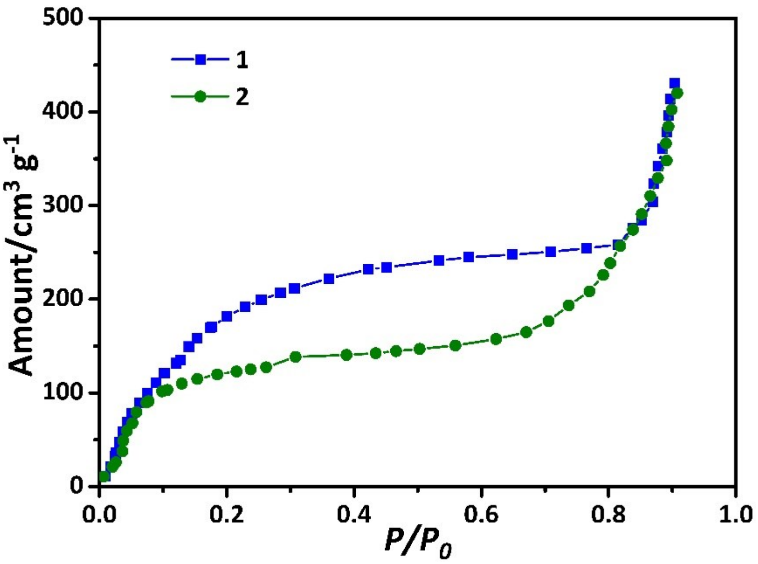

Fig. S9 Vapor sorption isotherms (298 K) of **1** and **2**.

Table S5 A summary of known vapor adsorption capacities of polyoxometalate materials and some well-known porous metal–organic frameworks (MOFs).

Compounds[a]	Amount/cm^3 g^{-1} (298 K, P/P_0 = 0.9)	Ref.
1	430.82	This work
2	420.09	This work
Mo_{240}	212	10
$H_9[Ln_9W_8(\mu_4\text{-}O)_{12}(\mu_2\text{-}O)_{24}(H_2O)_{24}](SiW_{12}O_{40})_3\cdot 60H_2O$ (Ln = La, Pr, Nd)	124.98; 114.79; 109.80	11
$\{K_4@\{[Cu_{29}(OH)_7(H_2O)_2(en)_8(trz)_{21}][H_2Nb_{24}O_{69}(H_2O)_3]_4\}\}^{30-}$	193	12
$\{[Cu(en)_2]\{[Cu_2(en)_2(trz)_2]_6(Nb_{68}O_{188})\}\}^{22-}$	188	12
$[Cu(en)_2]_6\{[Cu(en)_2]@\{[Cu_2(trz)_2(en)_2]_6[H_{10}Nb_{68}O_{188}]\}\}\cdot$solvent	224	12
$ILMo_{132}$	231.10	13
$HMeImMo_{132}$	186.20	13
$HImMo_{132}$	168.44	13
$\{[Cu(debpdc)(H_2O)_3][Cu(debpdc)(H_2O)Cl]$ $\text{-}[PMo_{12}O_{40}]\}\cdot 2CH_3OH\cdot 1.5CH_3CN\cdot 3H_2O$	98	14
$\{[Cu(H_2bpdc)(H_2O)_2Cl_{0.5}]_2[PW_{12}O_{40}]\}\cdot 10H_2O$	150	14
$\{[Cu(H_2bpdc)(H_2O)_{2.5}]_2[SiW_{12}O_{40}]\}\cdot 10H_2O$	92	14
$H_{14}[Na_6(H_2O)_{12}]_4[K_{42}Ge_8W_{72}O_{272}(H_2O)_{60}]\cdot$solvent	52	15
$A_2[Cr_3O(OOCH)_6(etpy)_3]_2[\alpha\text{-}SiW_{12}O_{40}]\cdot nH_2O$ (A = Li, Na, K, Cs,)	6–11	16
$[Co(pn)_3]_4[PNb_{12}O_{40}(VO)_6][OH]_5\cdot 20H_2O$	19.72	17

EB-COF:PW_{12}	78	18
$[Co(bpz)(Hbpz)][Co(SO_4)_{0.5}(H_2O)_2(bpz)]_4$-$[PMo^{VI}{}_8Mo^V{}_4V^{IV}{}_4O_{42}]\cdot13H_2O$ (NENU-530)	115	19
$[Ni_2(bpz)(Hbpz)_3(H_2O)_2][PMo^{VI}{}_8Mo^V{}_4V^{IV}{}_4O_{44}]\cdot8H_2O$ (NENU-531)	38	19
$Cu_6(Trz)_{10}(H_2O)4[H_2SiW_{12}O_{40}]\cdot8H_2O$	118	20
$K_2[Cr_3O(OOCH)_6(mepy)_3]_2[\alpha\text{-}PMo_{12}O_{40}]\cdot5H_2O$	56.8	21
$[Cu_3(\mu_3\text{-}OH)(H_2O)_3(atz)_3]_3[P_2W_{18}O_{62}]\cdot14H_2O$	28	22
$[Zn_{12}(trz)_{20}][SiW_{12}O_{40}]\cdot11H_2O$	150	23
$\{[Cu_4(dpdo)_{12}][H(H_2O)_{27}(CH_3CN)_{12}][PW_{12}O_{40}]_3\}_n$	65.1	24
$\{[Cu_3(L)_2(H_2O)_4]\ [Cu(dmf)_4(SiW_{12}O_{40})]\cdot9H_2O\}_n$	51.7	25
$H[Ni(Hbpdc)(H_2O)_2]_2[PW_{12}O_{40}]\cdot8H_2O\}$	31	26
$Cs_{3.6}K_{0.4}[PW_{11}O_{39}(Sn\text{-}OH)]\cdot8H_2O$	0.31	27
$Cs_3H_{0.3}[SiW_{12}O_{40}]_{0.83}\cdot3H_2O$	0.020	28
$K_2[Cr_3O(OOCH)_6(mepy)_3]_2[\alpha\text{-}SiW_{12}O_{40}]\cdot2H_2O\cdot CH_3OH$	0.03	29
$(DODA)_{23}[Mo_{154}O_{462}H_5]\cdot70H_2O$	16.6	30
$K_3[Cr_3O(OOCH)_6(H_2O)_3][\alpha\text{-}SiW_{12}O_{40}]$	130	31
$A_2[Cr_3O(OOCC_2H_5)_6(H_2O)_3]_2[\alpha\text{-}SiW_{12}O_{40}]\cdot nH_2O$ (A = K, Rb, NH_4, Cs)	18–23	32–35
MOF-801-SC; MOF-801-P; MOF-802; MOF-804; MOF-805; MOF-806; MOF-808; MOF-841 based on $\{Zr_6O_4(OH)_4(-CO_2)n\}$ secondary building units	350; 450; 110; 290; 410; 425; 735; 640	36
CAU-6; CAU-10; UiO-66;	380; 365; 535	36
ZIF-8	150	37

[a] Trz: 1,2,4-triazole; en: ethanediamine; IL: 1-(2-hydroxyethyl)-3-methylimidazolium; Im: imidazole; MeIm, 1-methylimidazolium; debpdc: diethyl 2,2′-bipyridine-4,4′-dicarboxylate; H_2bpdc: 2,2′-bipyridine-4,4′-dicarboxylic acid; etpy: 4-ethylpyridine; pn: 1,2-diaminopropane; H_2bpz: 3,3’,5,5’-tetramethyl-4,4’-bipyrazole; mepy: 4-methylpyridine; Hatz: 3-amino-1,2,4-triazolate; dpdo: 4,4′-bipyridine-N,N′-dioxide; L: *N*,*N*-bis[(2-hydroxy-3-methoxyphenyl)methylidene]hydrazine hydrate; dmf: N,N-dimethylformamide; DODA: dimethyldioctadecylammonium.

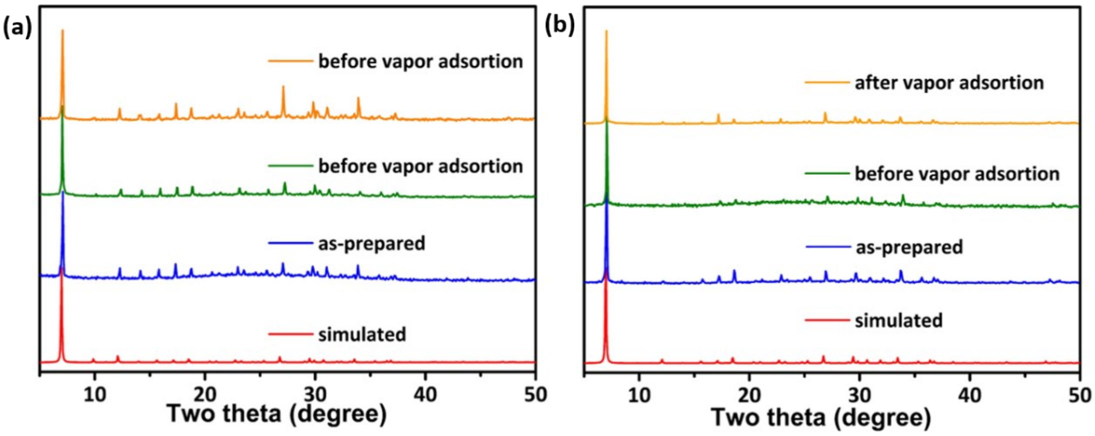

Fig. S10 PXRD patterns of (a) **1** and (b) **2**: simulated, experimental of as-synthesized samples, samples before and after vapor adsorption experiments.

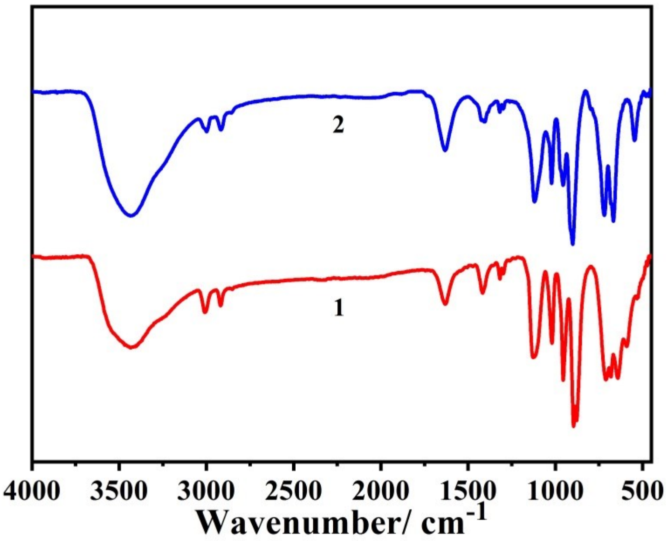

Fig. S11 IR spectra of **1** and **2**.

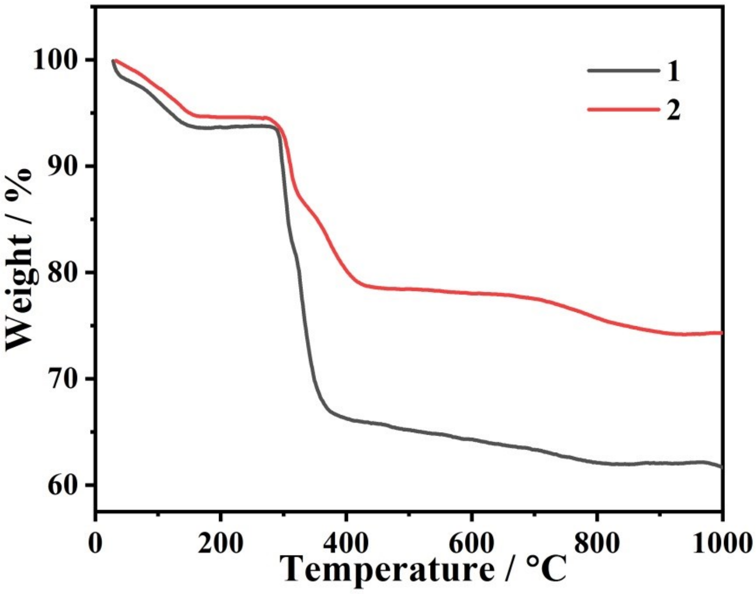

Fig. S12 TG curves of compound **1** and **2.**

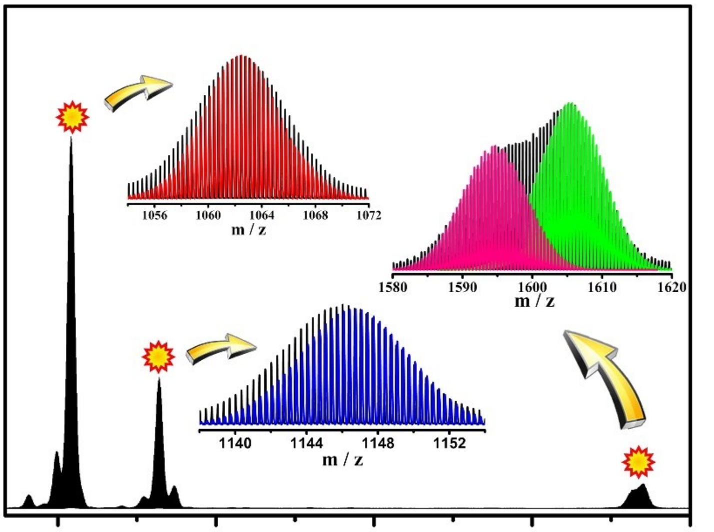

Fig. S13 Negative-mode ESI-MS spectrum of **1** in water. Inset: Experimental (black) and simulated (red, blue, pink and green lines) mass spectra of the isotopic envelopes for selected peaks. Here, three dominant ion series were observed, the former two are located at m/z = 1062.41(-3) and 1146.69(-3) corresponding to $\{[NaMo_{12}O_{42}(Ru(DMSO)_3)_4]\}^{3-}$ (cacld. 1062.67(-3)) and $\{[NaMo_{12}O_{42}(Ru(DMSO)_3)_4](H_2O)_{14}\}^{3-}$ (cacld. 1146.74(-3)) anions, respectively. The last bunch of small peaks centered at 1594.63(-2) and 1065.61(-2) were assigned to a overlapping pattern of two polyanions $\{H[NaMo_{12}O_{42}(Ru(DMSO)_3)_4]\}^{2-}$ (cacld. 1594.51(-2)) and $\{Na[NaMo_{12}O_{42}(Ru(DMSO)_3)_4]\}^{2-}$ (cacld. 1605.50(-2)). The monitoring of these species implied that the polyanion 1a can retain its key skeleton in water.

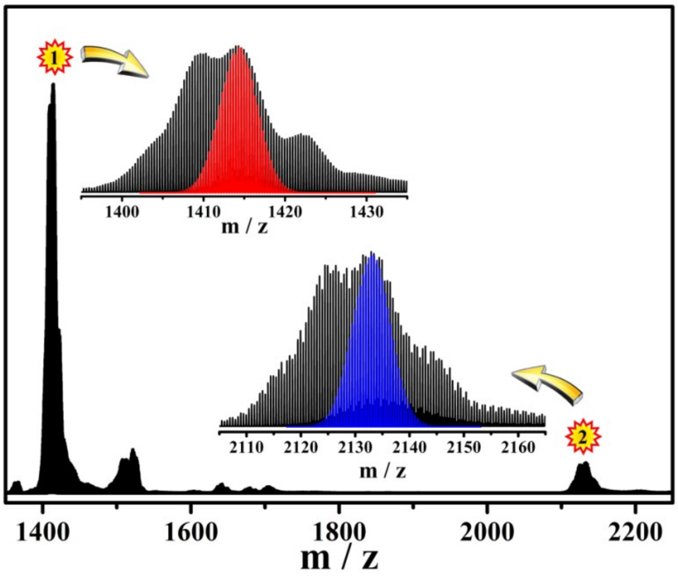

Fig. S14 Negative-mode ESI-MS spectrum of **2** in water. Inset: Experimental (black) and simulated (red, blue lines) mass spectra of the isotopic envelopes for selected peaks $\{[NaW_{12}O_{42}(Ru(DMSO)_3)_4]\}^{3-}$ (calcd. 1414.32(-3); found, 1414.29(-3)) and $\{Na[NaW_{12}O_{42}(Ru(DMSO)_3)_4]\}^{2-}$ (calcd. 2132.96(-2); found, 2132.93(-3)), respectively.

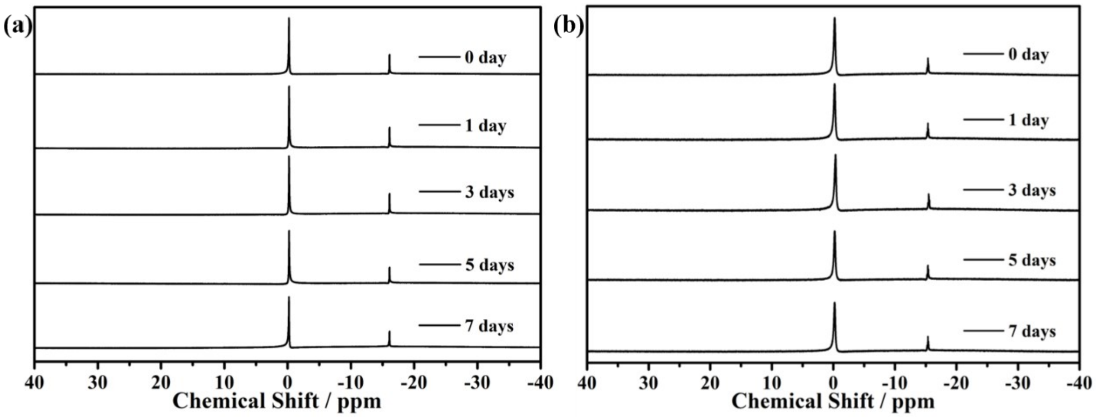

Fig. S15 Evolution of the ^{23}Na NMR spectra of (a) **1** and (b) **2** with time in D_2O.

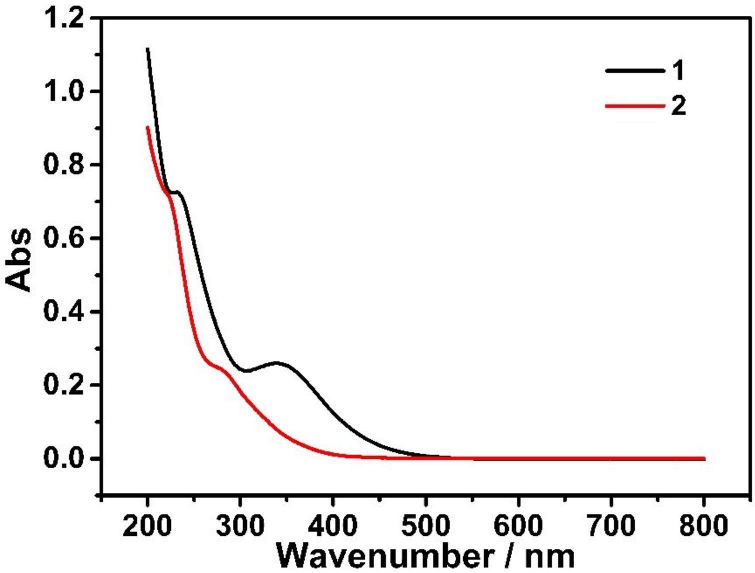

Fig. S16 UV-Vis spectra of **1** and **2** in H_2O.

REFERENCES

(1) L. Bi, F. Hussain, U. Kortz, M. Sadakane, M. H. Dickman, *Chem. Commun.*, 2004, **12**, 1420–1421.

(2) D. Barats-Damatov, L. J. W. Shimon, R. Neumann, *Eur. J. Inorg. Chem.*, 2013, **2013**, 1649–1653.

(3) SAINT, *Program for Data Extraction and Reduction*, Bruker AXS, Inc., Madison, WI, **2001**.

(4) (a) O. V. Dolomanov, L. J. Bourhis, R. J. Gildea, J. A. K. Howard, H. Puschmann, *J. Appl. Cryst.*, 2009, **42**, 339−341; (b) G. M. Sheldrick, *Acta Crystallogr., Sect. A: Found. Crystallogr.*, 2008, **64**, 112−122; (c) G. M. Sheldrick, *Acta Cryst.*, 2015, **A71**, 3−8; (d) G. M. Sheldrick, SHELXL-2018/3, Program for Crystal Structure Refinement, University of Göttingen, Germany, **2018**.

(5) D. D. Dexter, J. V. Silverton, *J. Am. Chem. Soc.*, 1968, **90**, 3589−3590.

(6) C.-D. Wu, C.-Z. Lu, H.-H. Zhuang, J.-S. Huang, *J. Am. Chem. Soc.*, 2002, **124**, 3836–3837.

(7) J. N. Cross, S. K. Cary, J. T. Stritzinger, M. J. Polinski, T. E. Albrecht Schmitt, *Inorg. Chem.*, 2014, **53**, 3148−3152.

(8) K. Bhattacharjee, K. K. Chattopadhyay, G. C. Das, *J. Phys. Chem. C*, 2015, **119**, 1536−1547.

(9) J. R. Günter, H. W. Schmalle, E. Dubler, *Solid State Ionics*, 1990, **43**, 85–92.

(10) Lin, N. Li, S. Yang, M. Jia, J. Liu, X.-M. Li, L. An, Q. Tian, L.-Z. Dong and Y.-Q. Lan, *J. Am. Chem. Soc.*, 2020, **142**, 13982–13988.

(11) J.-H. Liu, L.-D. Lin, G.-Q. Wang, L.-Y. Li, Y.-Q. Sun, X.-X. Li and S.-T. Zheng, *Chem. Commun.*, 2020, **56**, 10305–10308.

(12) Z. Zhu, Y. Lin, H. Yu, X. Li and S. Zheng, *Angew. Chem. Int. Ed.*, 2019, **58**, 16864–16868.

(13) W.-J. Liu, L.-Z. Dong, R.-H. Li, Y.-J. Chen, S.-N. Sun, S.-L. Li and Y.-Q. Lan, *ACS Appl. Mater. Interfaces*, 2019, **11**, 7030–7036.

(14) H. Yang, X.-Y. Duan, J.-J. Lai and M.-L. Wei, *Inorg. Chem.*, 2019, **58**, 1020–1029.

(15) Z. Li, L.-D. Lin, H. Yu, X.-X. Li and S.-T. Zheng, *Angew. Chem. Int. Ed.*, 2018, **57**, 15777–15781.

(16) S. Uchida, R. Hosono, R. Eguchi, R. Kawahara, R. Osuga, J. N. Kondo, M. Hibino and N.

Mizuno, *Phys. Chem. Chem. Phys.*, 2017, **19**, 29077–29083.

(17) J. Hu, Y. Xu, D. Zhang, B. Chen, Z. Lin and C. Hu, *Inorg. Chem.*, 2017, **56**, 10844–10847.

(18) H. Ma, B. Liu, B. Li, L. Zhang, Y.-G. Li, H.-Q. Tan, H.-Y. Zang and G. Zhu, *J. Am. Chem. Soc.*, 2016, **138**, 5897–5903.

(19) J. Li, X.-L. Cao, Y.-Y. Wang, S.-R. Zhang, D.-Y. Du, J.-S. Qin, S.-L. Li, Z.-M. Su and Y.-Q. Lan, *Chem. Eur. J.*, 2016, **22**, 9299–9304.

(20) E.-L. Zhou, C. Qin, P. Huang, X.-L. Wang, W.-C. Chen, K.-Z. Shao and Z.-M. Su, *Chem. Eur. J.*, 2015, **21**, 11894–11898.

(21) R. Kawahara, S. Uchida and N. Mizuno, *Chem. Mater.*, 2015, **27**, 2092–2099.

(22) Y.-Q. Jiao, H.-Y. Zang, X.-L. Wang, E.-L. Zhou, B.-Q. Song, C.-G. Wang, K.-Z. Shao and Z.-M. Su, *Chem. Commun.*, 2015, **51**, 11313–11316.

(23) E.-L. Zhou, C. Qin, X.-L. Wang, K.-Z. Shao and Z.-M. Su, *Chem. Eur. J.*, 2015, **21**, 13058–13064.

(24) M. Wei, L. Chen and X. Duan, *J. Coord. Chem.*, 2014, **67**, 2809–2819.

(25) M.-L. Wei, J.-J. Sun and X.-Y. Duan, *Eur. J. Inorg. Chem.*, 2014, **2014**, 345–351.

(26) M. Wei, X. Wang, J. Sun and X. Duan, *J. Solid State Chem.*, 2013, **202**, 200–206.

(27) Y. Miura, H. Imai, T. Yokoi, T. Tatsumi and Y. Kamiya, *Micropore. Mesopore. Mater.*, 2013, **174**, 34–43.

(28) Y. Ogasawara, S. Uchida, T. Maruichi, R. Ishikawa, N. Shibata, Y. Ikuhara and N. Mizuno, *Chem. Mater.*, 2013, **25**, 905–911.

(29) S. Uchida, R. Eguchi and N. Mizuno, *Angew. Chem. Int. Ed.*, 2010, **49**, 9930–9934.

(30) S. Noro, R. Tsunashima, Y. Kamiya, K. Uemura, H. Kita, L. Cronin, T. Akutagawa and T. Nakamura, *Angew. Chem. Int. Ed.*, 2009, **48**, 8703–8706.

(31) S. Uchida, R. Kawamoto and N. Mizuno, *Inorg. Chem.*, 2006, **45**, 5136–5144.

(32) A. Lesbani, R. Kawamoto, S. Uchida and N. Mizuno, *Inorg. Chem.*, 2008, **47**, 3349–3357.

(33) C. Jiang, A. Lesbani, R. Kawamoto, S. Uchida and N. Mizuno, *J. Am. Chem. Soc.*, 2006, **128**, 14240–14241

(34) R. Kawamoto, S. Uchida and N. Mizuno, *J. Am. Chem. Soc.*, 2005, **127**, 10560–10567.

(35) S. Uchida and N. Mizuno, *J. Am. Chem. Soc.*, 2004, **126**, 1602–1603.

(36) H. Furukawa, F. Gándara, Y.-B. Zhang, J. Jiang, W. L. Queen, M. R. Hudson and O. M. Yaghi, *J. Am. Chem. Soc.*, 2014, **136**, 4369–4381.

(37) P. Küsgens, M. Rose, I. Senkovska, H. Fröde, A. Henschel, S. Siegle and S. Kaskel, *Micropore. Mesopore. Mater.*, 2009, **120**, 325–330.